

Characterizing Scattering by 3-D Arbitrarily Shaped Homogeneous Dielectric Objects Using Fast Multipole Method

Jian-Ying Li, Le-Wei Li, *Senior Member, IEEE*

Abstract—Electromagnetic scattering by 3-D arbitrarily shaped homogeneous dielectric objects is characterized. In the analysis, the method of moments is first employed to solve the combined field integral equation for scattering properties of these three-dimensional homogeneous dielectric objects of arbitrary shape. The fast multipole method, and the multi-level fast multipole algorithm are implemented into our codes for matrix-vector manipulations. Specifically, four proposals are made and discussed to increase convergence and accuracy of iterative procedures (conjugate gradient method). Numerical results are obtained using various methods and compared to each other.

Index Terms—Electromagnetic scattering, Fast multipole method, method of moment.

I. INTRODUCTION

There have been a variety of numerical methods developed for studying electromagnetic scattering by dielectric objects, both asymptotically and numerically. Among those, the numerically exact methods include the method of moments (MoM), finite element method (FEM), finite-difference time-domain (FDTD) method, and their hybrid implementations. Among those numerical techniques, the surface integral equation approach is found to be very efficient to analyze homogeneous dielectric objects, therefore the MoM [1,2] is employed herein this paper. The MoM usually results in, however, a matrix of very large scale when applied to analyzing electrically large objects. In particular, approximately ten (or more) sub-sectional basis functions are generally required per wavelength; therefore, the number of unknowns, N , becomes quite large when scattering by an arbitrary general multi-wavelength, three-dimensional target is characterized. For the resultant matrix equation of N unknowns, the $O(N^3)$ floating-point operations are required in the Gaussian elimination; and the $O(N^2)$ operations are required in iterative method (such as the conjugate gradients method). Moreover, the memory requirements for a MoM solution are also to $O(N^2)$.

To overcome this, the fast multipole method (FMM), a well-known and popular technique, is used to speed up the MoM

solution of large-scale electromagnetic scattering and radiation problems [3-7]. It reduces both complexity of the matrix-vector multiplications and memory requirements to $O(N^{1.5})$. Multilevel fast multipole algorithm (MLFMA) is an extension of FMM [4] and can further reduce the computational complexity to $O(N \log N)$. In this paper, we explore the application of both the conjugate gradient method and the fast multipole method to 3-D dielectric objects of arbitrary shape. Particularly, emphasis is given to application of modified Rao-Wilton-Glisson (RGW) basis functions to reduce conditioning number of the resultant matrix in MoM procedure. This unique feature was realized in implementation of MoM into the FMM algorithm.

II. BRIEF DESCRIPTION OF FORMULATION AND ANALYSIS

Consider a 3-D homogeneous dielectric object of arbitrary shape shown in Fig. 1. It is characterized by a permittivity ϵ_2 and permeability μ_2 , immersed in an infinite and homogeneous medium having permittivity ϵ_1 and permeability μ_1 . The detailed derivation of the combined field integral equation can be found in [2]. For completeness, a summary of the CFIE is given below.

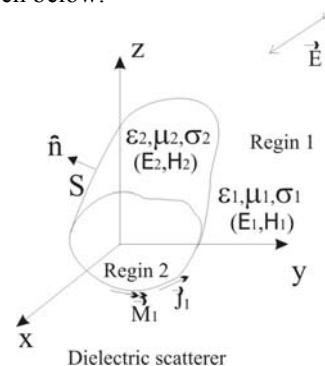


Fig. 1. Geometry of a dielectric scatterer in an infinite dielectric medium

Let the $\vec{J}(\vec{r})$ and $\vec{M}(\vec{r})$ represent the equivalent electric and magnetic currents on the surface of homogeneous object. Applying the equivalent principle to this electromagnetic problem and considering the boundary conditions, we obtain the electric and magnetic field integral equations as follows:

J. Y. Li is with the High Performance Computation for Engineered Systems (HPCES) Programme at Singapore-MIT (Massachusetts Institute of Technology) Alliance, Kent Ridge, Singapore 119620. (Email: smaliy@nus.edu.sg).

L. W. Li is with the Department of Electrical and Computer Engineering, National University of Singapore, Kent Ridge, Singapore 119620 (Web: <http://www.ece.nus.edu.sg/lwli>) and also with the HPCES Programme at Singapore-MIT Alliance, Kent Ridge, Singapore 119620. (Web: <http://web.mit.edu/sma>). E-mail lwli@nus.edu.sg.

$$\begin{aligned} \bar{E}'(\bar{r})|_{\text{tan}} = & \left\{ \left[j\omega\bar{A}_1(\bar{r}) + \nabla V_1(\bar{r}) \right] + \left[j\omega\bar{A}_2(\bar{r}) + \nabla V_2(\bar{r}) \right] \right. \\ & \left. + \left[\frac{1}{\varepsilon'_1} \nabla \times \bar{F}_1(\bar{r}) + \frac{1}{\varepsilon'_2} \nabla \times \bar{F}_2(\bar{r}) \right] \right\} |_{\text{tan}} \end{aligned} \quad (1a)$$

$$\begin{aligned} \bar{H}'(\bar{r})|_{\text{tan}} = & \left\{ \left[j\omega\bar{F}_1(\bar{r}) + \nabla U_1(\bar{r}) \right] + \left[j\omega\bar{F}_2(\bar{r}) + \nabla U_2(\bar{r}) \right] \right. \\ & \left. - \left[\frac{1}{\mu'_1} \nabla \times \bar{A}_1(\bar{r}) + \frac{1}{\mu'_2} \nabla \times \bar{A}_2(\bar{r}) \right] \right\} |_{\text{tan}} \end{aligned} \quad (1b)$$

for \bar{r} on the surface S , where $\bar{E}'(\bar{r})$ and $\bar{H}'(\bar{r})$ are the incident electric and magnetic fields in the region 1 and the subscript “tan” refers to as tangential components on the surface S . The vector potentials, $\bar{A}_i(\bar{r})$ and $\bar{F}_i(\bar{r})$ for $i=1,2$, and the scalar potentials, $V_i(\bar{r})$ and $U_i(\bar{r})$, are given by

$$\bar{A}_i(\bar{r}) = \frac{\mu_i}{4\pi} \int_S G_i(\bar{r}, \bar{r}') \cdot \bar{J}(\bar{r}') dS' \quad (2a)$$

$$\bar{F}_i(\bar{r}) = \frac{\varepsilon'_i}{4\pi} \int_S G_i(\bar{r}, \bar{r}') \cdot \bar{M}(\bar{r}') dS' \quad (2b)$$

$$V_i(\bar{r}) = \frac{1}{4\pi\varepsilon'_i} \int_S G_i(\bar{r}, \bar{r}') \cdot \rho^e(\bar{r}') dS' \quad (2c)$$

$$U_i(\bar{r}) = \frac{1}{4\pi\mu_i} \int_S G_i(\bar{r}, \bar{r}') \cdot \rho^m(\bar{r}') dS' \quad (2d)$$

$$\varepsilon'_i = \varepsilon_i - j\sigma_i/\omega \quad (2e)$$

$$\rho^e(\bar{r}') = \frac{-1}{j\omega} \left[\nabla' \cdot \bar{J}(\bar{r}') \right] \quad (2f)$$

$$\rho^m(\bar{r}') = \frac{-1}{j\omega} \left[\nabla' \cdot \bar{M}(\bar{r}') \right]. \quad (2g)$$

The Green's functions, $G_i(\bar{r}, \bar{r}')$ for $i=1,2$, have the form of

$$G_i(\bar{r}, \bar{r}') = \frac{e^{-jk_i R}}{R} \quad (3)$$

where

$$R = |\bar{r} - \bar{r}'| \quad \text{and} \quad k_i = \omega\sqrt{\mu_i\varepsilon'_i}. \quad (4)$$

As in a conventional MoM solution, the unknown surface electric and magnetic currents, $\bar{J}(\bar{r})$ and $\bar{M}(\bar{r})$, are expanded into two sets of basis functions, $\{\bar{J}_n(\bar{r})\}$ and $\{\bar{M}_n(\bar{r})\}$, below:

$$\bar{J}(\bar{r}) = \sum_{n=1}^N I_n \bar{J}_n(\bar{r}) \quad (5a)$$

$$\bar{M}(\bar{r}) = \sum_{n=1}^N M_n \bar{M}_n(\bar{r}) \quad (5b)$$

where N denotes the total number of edges on S , $\bar{J}_n(\bar{r})$ stands for the RWG vector basis functions [2], and I_n and M_n are the unknown expansion coefficients.

Substituting (5a) and (5b) into (1a) and (1b), and testing the CFIEs in (1a) and (1b) with a set of weighting functions

$\{\bar{f}_n(\bar{r})\}$ tangential to the scatterer's surface will result in $2N$ linear equations written in matrix form

$$\left[Z_{ij}^{1JJ} + Z_{ij}^{2JJ} \right] [I_j] + \left[Z_{ij}^{1MJ} + Z_{ij}^{2MJ} \right] [M_j] = [E_i] \quad (6a)$$

$$\left[Z_{ij}^{1JM} + Z_{ij}^{2JM} \right] [I_j] + \left[Z_{ij}^{1MM} + Z_{ij}^{2MM} \right] [M_j] = [H_i] \quad (6b)$$

where

$$\begin{aligned} Z_{ij}^{1JJ} = & \frac{j\omega\mu_1}{4\pi} \int_S \bar{f}_i(\bar{r}') \int_S G_1(\bar{r}, \bar{r}') \cdot \bar{f}_j(\bar{r}') dS' dS \\ & + \frac{1}{4\pi j\omega\varepsilon'_1} \int_S \left(\nabla \cdot \bar{f}_i(\bar{r}') \right) \int_S G_1(\bar{r}, \bar{r}') \cdot \left(\nabla' \cdot \bar{f}_j(\bar{r}') \right) dS' dS \end{aligned} \quad (7a)$$

$$\begin{aligned} Z_{ij}^{1MJ} = & \frac{-1}{4\pi} \int_S \bar{f}_i(\bar{r}') \int_S \nabla' G_1(\bar{r}, \bar{r}') \times \bar{f}_j(\bar{r}') dS' dS \\ = & -Z_{ij}^{1JM} \end{aligned} \quad (7b)$$

$$\begin{aligned} Z_{ij}^{1MM} = & \frac{j\omega\varepsilon'_1}{4\pi} \int_S \bar{f}_i(\bar{r}') \int_S G_1(\bar{r}, \bar{r}') \cdot \bar{f}_j(\bar{r}') dS' dS \\ & + \frac{1}{4\pi j\omega\mu_1} \int_S \left(\nabla \cdot \bar{f}_i(\bar{r}') \right) \int_S G_1(\bar{r}, \bar{r}') \cdot \left(\nabla' \cdot \bar{f}_j(\bar{r}') \right) dS' dS \end{aligned} \quad (7c)$$

$$E_i = \int_S \bar{f}_i(\bar{r}) \cdot \bar{E}'(\bar{r}) dS \quad (8)$$

$$H_i = \int_S \bar{f}_i(\bar{r}) \cdot \bar{H}'(\bar{r}) dS. \quad (9)$$

The sub-matrixes, Z_{ij}^{2JJ} , Z_{ij}^{2JM} , Z_{ij}^{2MJ} , and Z_{ij}^{2MM} , can be also obtained, provided that all the superscripts in (7) are changed from “1” to “2”.

The electric and magnetic currents' expansion coefficients, I_n and M_n , can be obtained directly using the Gaussian elimination method for small object. But for large objects, the iterative method (for instance, the conjugate gradients method) is desirable. In this case where the matrix can be ill-conditioning, therefore, the convergence becomes an important issue that we will address herein. For improving the conditioning number of the matrix in (6), we propose four different ways to overcome the magnetic current expansion coefficients, I_n and M_n :

- ✓ A: using matrix equations in (6a) and (6b) directly;
- ✓ B: multiplying $(-\eta_0)$ to both sides of (6b);
- ✓ C: expanding $\bar{M}(\bar{r})$ into a set of modified basis functions below
$$\bar{M}(\bar{r}) = \sum_{n=1}^N M_n [\eta_0 \cdot \bar{f}_n(\bar{r})]; \quad (10)$$
- ✓ D: expanding $\bar{M}(\bar{r})$ like in Method C and multiplying $(-\eta_0)$ to both sides of (6b).

III. ANALYSIS USING FMM AND MLFMA

In the FMM analysis [3,4], fields are divided into “near” and “far” terms according to interactions between the source point and the field point. The “near” interactions are handled using the MoM while the “far” interactions are processed applying the addition theorem to free-space scalar Green's function. As discussed previously, the FMM and its extension MLFMA

have been applied successfully to electromagnetic scattering by various electric-type perfectly conducting objects in free space [3-5]. For a dielectric object, eight formulas are obtained using FMM. The basic formulas in FMM based on Method D are given below:

$$Z_{ij}^{1JJ} = \frac{\omega\mu_1 k_1}{16\pi^2} \int d^2\hat{k} V_{1mj}(\hat{k}) \alpha_1(\vec{k}, \vec{r}_{mm'}) V_{1m'i}(\hat{k}) \quad (11)$$

$$Z_{ij}^{1MM} = \frac{\omega\varepsilon_1' k_1 \eta_0^2}{16\pi^2} \int d^2\hat{k} V_{1mj}(\hat{k}) \alpha_1(\vec{k}, \vec{r}_{mm'}) V_{1m'i}(\hat{k}) \quad (12)$$

$$Z_{ij}^{1JM} = \frac{k_1 \eta_0}{16\pi^2} \int d^2\hat{k} V_{D1mj}(\hat{k}) \alpha_1(\vec{k}, \vec{r}_{mm'}) V_{1m'i}(\hat{k}) = Z_{ij}^{1MJ} \quad (13)$$

where

$$V_{1mj}(\hat{k}) = \int_S (\mathbf{I} - \hat{k}\hat{k}) \cdot \vec{f}_j(\vec{r}) e^{-i\vec{k} \cdot (\vec{r} - \vec{r}_m)} dS \quad (14)$$

$$V_{D1mj}(\hat{k}) = \int_S e^{-i\vec{k} \cdot (\vec{r} - \vec{r}_m)} \hat{k} \times \vec{f}_j(\vec{r}) dS \quad (15)$$

$$V_{1m'i}(\hat{k}) = \int_S \vec{f}_i(\vec{r}) e^{i\vec{k} \cdot (\vec{r} - \vec{r}_{m'})} dS \quad (16)$$

$$\alpha_1(\vec{k}, \vec{r}_{mm'}) = \sum_{l=0}^L (-i)^l (2l+1) h_l^{(2)}(k_1 \cdot r_{mm'}) P_l(\hat{k} \cdot \hat{r}_{mm'}) \quad (17)$$

$$\int (\bullet) d^2\hat{k} = \iint_S (\bullet) \sin\theta d\theta d\varphi, \quad (18)$$

$$\hat{k} = (\sin\theta \cos\varphi, \sin\theta \sin\varphi, \cos\theta). \quad (19)$$

In the above formulas, \vec{r}_m denotes the center of the m th group (where $\vec{r}_{mm'} = \vec{r}_m - \vec{r}_{m'}$), $h_l^{(2)}$ identifies a spherical Hankel function of the second kind, P_l stands for a Legendre polynomial of degree l , and L denotes the number of multipole expansion terms [6]. Also, Z_{ij}^{2JJ} , Z_{ij}^{2MM} , Z_{ij}^{2JM} , Z_{ij}^{2MJ} , V_{2mj} , V_{D2mj} , $V_{2m'i}$, and $\alpha_2(\vec{k}, \vec{r}_{mm'})$ can be obtained from (11)-(17) by changing sub- and super-scripts from “1” to “2”.

In the MLFMA, the same idea is used to characterize dielectric objects. Based on the FMM formulas given above, the MLFMA can be implemented for the dielectric objects as described in [4]. Subsequently, we will show some numerical examples for which we have developed our own FMM algorithms which cannot be obtained elsewhere.

IV. RESULTS

To compare among these four techniques, we first consider a dielectric sphere in free space whose $ka = 3.14$. Its relative permittivity and permeability are 4 and 1, respectively. Fig. 2 depicts the normalized residual norm in the CG method as functions of the number of iterations for Methods A, B, C, and D. It is found that Method D converges very much faster than Methods A, B, and C. This suggests the Method D instead of the conventional Method A and other alternatives.

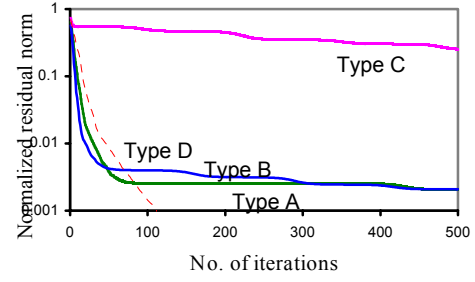


Fig. 2. Convergence of solutions to a dielectric sphere of $ka = 3.14$ using Methods A-D (3398 unknowns).

Also, we obtain their corresponding RCS results shown in Fig. 3. The RCS result obtained by Method D agrees very well with the Mie theory result, but the results by Methods A, B, and C are not good at all.

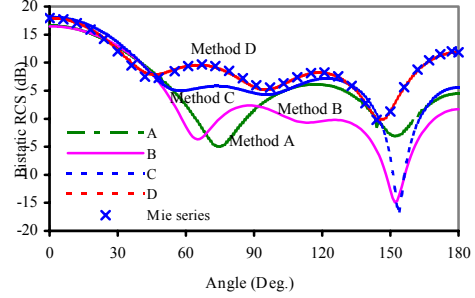


Fig. 3. Bistatic RCS of dielectric sphere whose $ka = 3.14$ (3398 unknowns).

To further check and confirm our observation, we consider another example, that is, a semi-spherical dielectric bowl shown in Fig. 4. The outer radius and inner radius of this dielectric bowl are 1 m and 0.8 m, respectively. Its relative permittivity and permeability are 4 and 1, respectively.

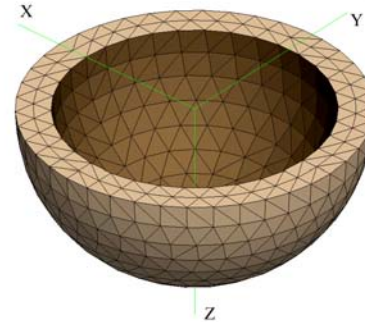


Fig. 4. Structure of a dielectric semi-sphere bowl whose inner and outer radii are 0.8 m and 1 m, respectively.

Subsequently, consider a plane wave incident at an angle of $\theta = 0^\circ$ and $\phi = 0^\circ$. Again, the normalized residual norm used in the CG method is obtained and shown in Fig. 5 as functions of the number of iterations based on the four methods at $f = 150$ MHz. It is further confirmed that Method D is still the best choice among the four proposals. This means that to speed up

the matrix-vector manipulations in the method of moments, it is best to employ Method D. To check the accuracy of the results, the bistatic RCS of this dielectric semi-sphere bowl is shown in Fig. 6. And a comparison of the results between the iterative method and Gaussian elimination method is shown and a good agreement is obtained. It again verifies our conclusion.

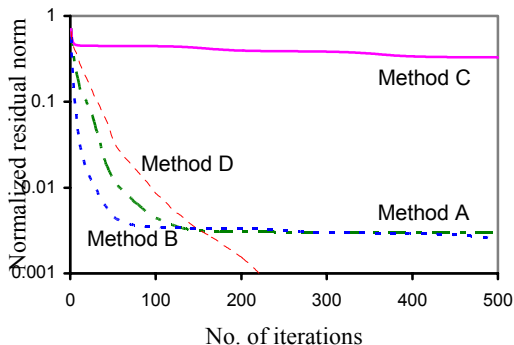


Fig. 5. Convergence test for a dielectric semi-spherical bowl using Methods A-D at $f = 150$ MHz (4068 unknowns).

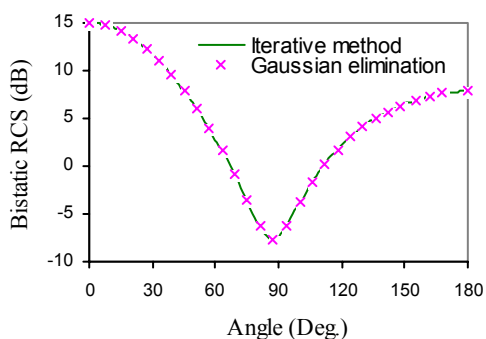


Fig. 6. Bistatic RCS of a semi-sphere dielectric bowl (Incident angle: $\theta = 0^\circ, \phi = 0^\circ$)

Fig. 7 shows the bistatic RCS of a dielectric sphere whose $ka = 3.14$ and for which 3398 unknowns are assumed in our FMM. The RCS results are compared to those obtained using the MoM and Mie theory and a good agreement is observed.

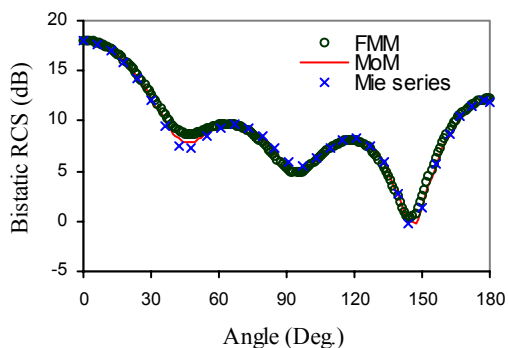
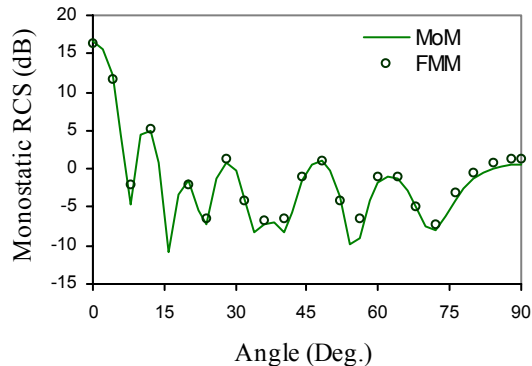
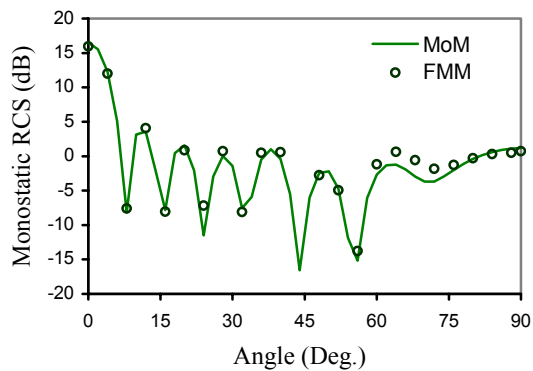


Fig. 7. Bistatic RCS of dielectric sphere whose $ka = 3.14$ (where there are 3398 unknowns).

Also, Fig. 8 shows the monostatic RCSs obtained using FMM and the standard MoM for a lossy dielectric box having dimensions of $3.5\lambda \times 2.0\lambda \times 0.25\lambda$ and relative permittivity and permeability of $3 - 0.09i$ and 1, respectively. The incident angle is assumed to be at $\phi = 0^\circ$ plane. It is seen that both results are very close for both polarizations.



(a) $\phi\phi$ -polarization



(b) $\theta\theta$ -polarization

Fig. 8 Monostatic RCS of a lossy dielectric box where $\epsilon_r = 3 - 0.09i$ and at $\phi = 0^\circ$ incident angle.

V. CONCLUSION

In this work, electromagnetic scattering by 3D arbitrarily shaped homogeneous dielectric objects is characterized using the MoM together with CG method, FMM, and MLFMA. In the Galerkin's procedure, the RWG functions as used as both basis and test functions. Also, four proposals are made for improving the conditioning number of the matrix so as to increase the convergence and accuracy of the solution to the CFIE. It is realized that only Method D among the four proposals results in fast convergence and high accuracy. Furthermore, the FMM formulas based on Method D are made and some numerical results of RCSs are obtained using the FMM and MLFMA.

ACKNOWLEDGMENT

This work has been supported by Temasek Laboratories, National University of Singapore (NUS). The authors are grateful to Dr. M. Zhang, Dr. C.-F. Wang, Dr. N. Yun and Dr. X.-C. Nie for their. Acknowledgment also goes to Prof.

W.C. Chew who provided some useful suggestions.

REFERENCES

- [1] S. M. Rao, D. R. Wilton, and A. W. Glisson, "Electromagnetic Scattering by Surfaces of Arbitrary Shape," *IEEE Trans. Antennas Propagat.*, vol. AP-30, no. 3, pp. 409–418, May 1982.
- [2] K. Umashankar, A. Taflove, and S. M. Rao, "Electromagnetic Scattering by Arbitrary Shaped Three- Dimensional Homogeneous Lossy Dielectric Objects," *IEEE Trans. Antennas Propagat.*, vol. AP-34, no. 6, pp. 758–766, June 1986.
- [3] R. Coifman, V. Rokhlin, and S. Wandzura, "The fast multipole method FMM for the wave equation: A pedestrian prescription," *IEEE Antennas Propagat. Magazine*, vol. 35, no. 3, pp. 7-12, June 1993.
- [4] J. M. Song and W. C. Chew, "Multilevel fast-multipole algorithm for solving combined field integral equations of electromagnetic scattering," *Microwave Opt. Technol. Lett.*, vol. 10, no.1, pp. 14-19, 1995.
- [5] K. Sertel and J. L. Volakis, "The effect of FMM parameters on the solution of PEC scattering problems," *IEEE Int. Symp. Antennas Propagat. Dig.*, Orlando, FL, pp. 624-627, 1999.
- [6] J. Y. Li, L. W. Li, B. L. Ooi, P. S. Kooi, and M. S. Leong, "On accuracy of addition theorem for scalar Green's function used in FMM," *Microwave Optical Technol. Lett.*, vol. 31, no. 6, pp. 439-442, 2001.
- [7] X. Q. Sheng, J. M. Jin, J. M. Song, W. C. Chew, and C. C. Lu, "Solution of combined-field integral equation using multievel fast multipole algorithm for scattering by homogeneous bodies," *IEEE Trans. Antennas Propagat.*, vol. AP-46, no. 11, November 1998 , pp. 1718-1726.
- [8] S. J. Zhang and J. M. Jin, *Computation of Special Function*, Wiley: New York, 1995.